Mechanistic facets of the competition between cross-coupling and homocoupling in supporting ligand-free iron-mediated aryl–aryl bond formations

Edouard Zhou, Pablo Chourreu, Nicolas Lefèvre, Mathieu Ahr, Lidie Rousseau, Christian Herrero, Eric Gayon, Gérard Cahiez, Guillaume Lefèvre

Mechanistic facets of the competition between cross-coupling and homo-coupling in supporting ligand-free iron-mediated aryl-aryl bond formations.

Edouard Zhou,[b,c]# Pablo Chourreu,[a,c]# Nicolas Lefèvre,[b] Mathieu Ahr,[b] Lidie Rousseau,[a,d] Christian Herrero,[e] Eric Gayon,[c] Gérard Cahiez,[b] and Guillaume Lefèvre*[a]*

[a] Chimie ParisTech, PSL University, CNRS, Institute of Chemistry for Life and Health Sciences, CSB2D, 75005 Paris, France.

[b] Institut de Recherche de Chimie Paris, CNRS UMR8247, Chimie ParisTech, PSL Research University, 11 rue Pierre et Marie Curie, 75005 Paris, France.

[c] M2i Development, Bâtiment ChemStart'Up, 64170 Lacq, France.

[d] Université Paris-Saclay, CEA, CNRS, NIMBE, 91191 Gif-sur-Yvette cedex, France.

[e] Institut de Chimie Moléculaire et des Matériaux d'Orsay (UMR 8182) Univ. Paris Sud, Université Paris Saclay 91405 Orsay cedex (France)

# equal contributions.

ABSTRACT

In the context of cross-coupling chemistry, the competition between the cross-coupling path itself and the oxidative homocoupling of the nucleophile is a classic issue. In that case, the electrophilic partner acts as a sacrificial oxidant. We investigate in this report the factors governing the cross- versus homocoupling distribution using aryl nucleophiles ArMgBr and (hetero)aryl electrophiles Ar'Cl in the presence of an iron catalyst. When electron-deficient electrophiles are used, a key transient heteroleptic $[Ar_2Ar'Fe^{II}]^-$ complex is

formed. DFT calculations show that an asynchronous 2-electron reductive elimination follows, which governs the selective evolution of the system towards either cross- or homocoupling product. Proficiency of the cross-coupling reductive elimination strongly depends on both π-accepting and σ-donating effects of the Fe^{II}-ligated Ar' ring. The reactivity trends discussed in this article rely on 2-electron elementary steps, which are in contrast with the usually described tendencies in iron-mediated oxidative homocouplings which involve single-electron transfers. Those results have been probed by paramagnetic ^{1}H NMR spectroscopy, experimental kinetics data and DFT calculations.

KEYWORDS. iron catalysis • cross-coupling • homocoupling • two-electron processes • kinetics • mechanisms

INTRODUCTION

In the field of transition-metal-catalyzed transformations, Fe-mediated cross-couplings have been intensely developed in the last decades, thanks to the pioneer work of Kochi,[1,2] Cahiez,[3] Fürstner,[4,5] Nakamura[6,7] and Bedford.[8-10] Thanks to its abundance and its good eco-compatibility, this cheap metal led to a significant breakthrough in transition-metal catalysis.[11-14] Moreover, its rich redox chemistry (with a formal oxidation state panel ranking from Fe^{-II} to Fe^{+VI}) opens the way to a huge variety of reactivity patterns, involving both 1- and 2-electron redox chemistry.[15] From a synthetic standpoint, the classic procedures of Fe-mediated couplings between Grignard reagents and organic halides developed by Cahiez and later on by Fürstner are particularly appealing since they allow the obtention of high yields using simple ferrous or ferric salts as catalysts in the absence of additional ligands, with THF:NMP solvent mixtures (FeX_n, $Fe(acac)_n$ (X = Br, Cl; n = 2, 3)).[3,4]

However, the use of simple iron salts as catalysts also leads in several cases to a broad distribution of byproducts. When aryl nucleophiles are used as coupling partners, notable quantities of homocoupled bisaryls can also be formed (Scheme 1a).[8] Formation of this side-product thus hampers a full conversion of the reactant, limiting the possible extension of those methods to industrial processes. A fine understanding of the redox events undergone by the iron catalyst during the catalytic process is thus highly desirable to finally control more efficiently the factors governing the formation of homocoupling byproducts.

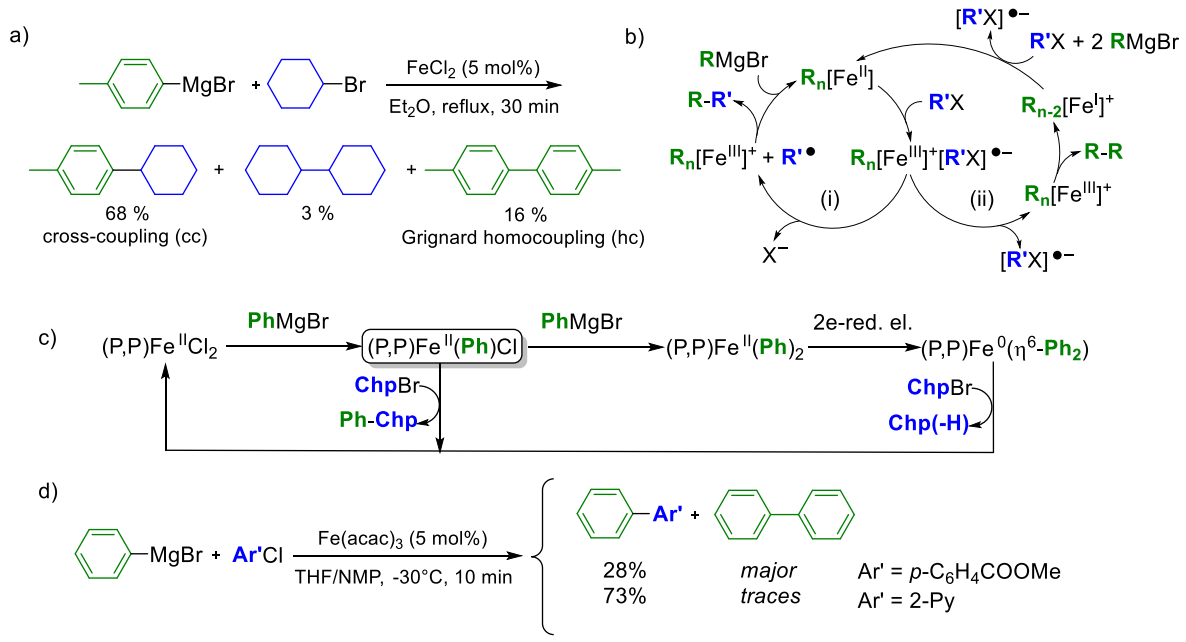

Scheme 1: a) distribution of cross- and homocoupled products in an aryl-alkyl system developed by Bedford; b) general scheme of the cross-coupling (i) and homocoupling (ii) catalytic cycles relying on a one-electron process involving the Fe^{II} / Fe^{III} couple; c) off-cycle homocoupling process in an aryl-alkyl coupling system mediated by the Fe^{0} / Fe^{II} couple (Chp = cycloheptyl; (P,P) = SciOPP = 1,2-C_6H_4($(3,5\text{-}C_6H_3t Bu_2)_2P)_2$); d) representative example of a cross- *versus* homocoupling competition depending on the nature of the electrophilic partner.

From a mechanistic standpoint, the active iron oxidation state in a cross-coupling cycle strongly depends on the nature of the coupling partners. For example, organoiron(II) intermediates proved to be often highly reactive towards alkyl halides, initiating the coupling cycle by a single electron transfer (SET) step. The catalytic cycle thus features a Fe^{II} / Fe^{III} redox couple (Scheme 1b).[14] In that case, oxidation of an on-cycle organoiron(II) intermediate by the electrophilic partner R'-X affords a transient organoiron(III) species along with radical R'•. A radical rebound of those species allows to close the cross-coupling cycle (Scheme 1b, path i). On the other hand, homocoupling of the nucleophile can also occur from the organoiron(III) intermediate in a second catalytic process, in which the organic halide acts as a sacrificial oxidant (path ii). Alternatively, multiple transmetallations of the nucleophile onto on-cycle Fe^{II} species can also lead to sacrificial homocoupling of the

former along with a Fe^0 complex (Scheme 1c). In that case, the organic electrophile acts as a sacrificial oxidant allowing the regeneration of the Fe^{II} precatalyst from the reduced Fe^0 species. This mechanism has been probed by Neidig in the aryl-alkyl cross-coupling using a diphosphino-ligated $(P,P)Fe^{II}Cl_2$ as resting state, system in which a bis-aryliron(II) intermediate $(P,P)Fe^{II}(Ph)_2$ undergoes a 2-electron reductive elimination leading to the formation of a biphenyle molecule ligated to a Fe^0 center. The latter species then reaffords the precatalyst $(P,P)Fe^{II}Cl_2$ after oxidation by the electrophilic partner (herein Chp-Br, bromocycloheptane), this step mostly affording the β-elimination product (cycloheptene).[16] It must also be stated that in the absence of well-defined exogenous ligand, several multinuclear species formed by reduction of $Fe(acac)_3$ with PhMgBr were structurally characterized, such as the ferrous dinuclear complex $[Mg(acac)(THF)_4]_2[FePh_2(\mu\text{-}Ph)]_2 \cdot 4THF$ as well as the tetranuclear species $Fe_4(\mu\text{-}Ph)_6(THF)_4$. The latter cluster is a rare example of a reduced iron species (with an average oxidation state lower than +II) displaying a catalytic activity in a cross-coupling involving aliphatic halides.[17]

In terms of harsh competition between the cross-coupling path and the off-cycle homocoupling process, the example of the aryl-aryl cross-coupling series is particularly illustrative. Selective formation of aryl-aryl cross-coupling products has remained a challenge for a long time, the bisaryl originating from the homocoupling of the nucleophilic partner being often obtained as the major compound. This point was described by Kharasch during the 1940s in a series of reports, showing that aryl halides with a significantly high oxidative power acted as sacrificial oxidants in transition-metal promoted Grignard oxidative homocoupling. Simple halide salts such as $FeCl_3$, $CoCl_2$ or $NiCl_2$ were used as catalysts for those transformations.[18] This point was later on confirmed by Fürstner, who reported efficient aryl-heteroaryl couplings involving heteroaryl chlorides as coupling partners, procedures which are difficultly applicable to more easily reduced substrates such as electron-poor aryl chlorides, e.g. methyl 4-chlorobenzoate (in the latter case, the oxidative homocoupling of the Grignard reagent is the preferred path).[4] This representative example is detailed in Scheme 1d. Amongst the scarce successful reported iron-mediated cross aryl-aryl bond formations, Knochel reported that use of arylcopper nucleophiles, weaker than their Mg-based analogues, and aryl iodides substituted by electron-withdrawing groups associated with $Fe(acac)_3$ catalyst mostly led to the expected cross-coupling product.[19] Nakamura reported a more general procedure allowing the suppression of the Grignard bisaryl in aryl-aryl cross-coupling

systems using FeF_3 as a catalyst combined with a N-Heterocyclic Carbene (NHC) ligand.[20] Similarly, Duong described an association of NHC ligands and alkoxide salts leading to efficient Fe-catalyzed aryl-aryl cross-couplings.[21]

The competition between cross-coupling and Grignard oxidative homocoupling paths promoted by transition metal catalysts in the presence of strongly oxidant aryl halides has been well documented since the work of Kharasch. Under reducing conditions, it has been demonstrated in several cases that low-valent iron complexes acted as one-electron reductants of Ar-X bonds (X = Cl, Br, I) in single-electron transfer (SET) steps, leading to the formation of the corresponding C-C coupled products by a formal radical dimerization. Bis(2-halophenyl)methylamines (in the chloro and bromo series) were thus converted into the corresponding carbazole using strongly reductive iron *ate* complexes generated by action of MeLi onto iron precursors in the presence of Mg metal.[22] However, much less is known regarding the reactivity trends of similar systems involving less reducing iron intermediates, which difficultly promote single-electron transfers. In a recent work, we demonstrated that (hetero)aryl halides Ar'Cl such as C_6F_5Cl and 2-chloropyridine (2-PyCl) could be activated by transient Fe^0 complexes in a 2-electron oxidative addition process in the presence of aryl Grignard reagents ArMgBr to afford well-defined heteroleptic species $[Ar_2Ar'Fe^{II}]^-$.[23] In that case, the reactive Fe^0 intermediate is generated by reduction of iron precursors using an excess of PhMgBr. This bielectronic activation is particularly interesting in the case of C_6F_5Cl, whose first reduction potential (E_{red} = -2.05 V *vs* SCE)[24] is close to that of other aryl chlorides (e.g. ethyl 4-chlorobenzoate, E_{red} = -2.02 V *vs* SCE)[25], which traditionally act as monoelectronic sacrificial oxidants.[1-10,22] Owing to its more negative reduction potential (E_{red} = -2.37 V *vs* SCE),[25] 2-PyCl displays a less pronounced tendency to undergo one-electron reduction events.

This prompted us to investigate the mechanistic aspects of classic aryl-aryl bond formation systems following this 2-electron reactivity pattern, with a particular focus on the factors governing the competition between the formation of the cross-coupling (cc) and the homocoupling (hc) products. We demonstrate in this work that the reactivity of both C_6F_5Cl and 2-PyCl in the presence of aryl nucleophiles and of an iron catalyst is driven by 2-electron processes, regardless of the preferred path (selective oxidative homocoupling of the aryl nucleophile in the presence of C_6F_5Cl, or possible formation of a cross-coupling product using 2-PyCl). The selectivity

displayed by the system for one path or the other is on the other hand strongly influenced by the nature of the electronic effects governing the reactivity of the Ar / Ar' couple. Those results are sustained by experimental kinetics experiments as well as by DFT calculations.

RESULTS AND DISCUSSION

Oxidative homocoupling in the presence of an aryl halide as a sacrificial oxidant. Iron-catalyzed oxidative homocoupling of aromatic Grignard reagents can be performed in excellent yields via several procedures, which require sacrificial oxidants. Some of us already described in the past an iron-catalyzed oxidative homocoupling reaction using atmospheric oxygen (Scheme 2).[26]

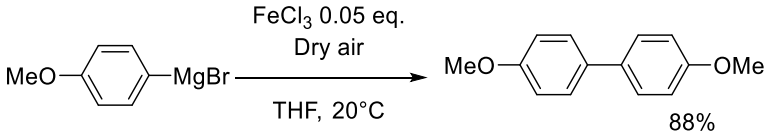

Scheme 2 : oxidative homocoupling of an aryl Grignard reagent mediated by $FeCl_3$ in the presence of O_2 as sacrificial oxidant.

The methodology described in Scheme 2 is thus a very convenient way to prepare symmetric bisaryls from the corresponding Grignard reagents (ArMgBr) using a cheap and abundant sacrificial oxidant. From a mechanistic standpoint, a first one-electron reduction of the Fe^{III} precursor by ArMgBr usually occurs, leading to the formation of the Fe^{II} oxidation state.[27] The final bisaryl is then obtained after a 2-electron reductive elimination of a transient *in situ* generated organoiron(II) species with a transmetallation degree Ar : Fe > 1, such as a *ate* $[Ar_3Fe^{II}]^-$ complex.[28] The reduced iron species obtained after this step is then reoxidized at the Fe^{II} stage by the sacrificial oxidant (O_2 herein), which initiates a new catalytic cycle.

In a cross-coupling context though, the classic methodology consists in promoting a C-C bond formation between an organometallic nucleophile (e.g. ArMgBr in the aromatic series) and an organic electrophile (usually a halide or a pseudo-halide). As outlined in the introduction of this article, bisaryls Ar-Ar are commonly

obtained as side-products in a parallel catalytic homocoupling process, the organic halide playing likely the role of a monoelectronic sacrificial oxidant. The reactivity of C_6F_5Cl and 2-PyCl towards a scope of aryl Grignard reagents in the presence of an iron catalyst ($FeCl_3$ or $Fe(acac)_3$) was then examined and a particular focus was put on the analysis of the cross-coupling versus homocoupling ratio. As outlined in the introduction, the choice of those substrates was motivated by their ability to undergo 2-electron activation processes. $FeCl_3$ and $Fe(acac)_3$ were chosen for this benchmark work since they are amongst the most used ferric precatalysts in Fe-mediated coupling chemistry. Both were moreover used successfully by Fürstner or Cahiez in several coupling systems.[3,4] Very poor yields are obtained in cross-coupling attempts using C_6F_5Cl (Table 1), and the oxidative homocoupling of the nucleophile is observed, almost quantitatively in some cases (**2a**, Entry 2). On the other hand, the use of 2-chloropyridine (2-PyCl) as a coupling partner resulted in a more productive cross-coupling pathway, since up to 22% of cross-coupling product **6b** is obtained when *p*-Me_2N-C_6H_4MgBr is used as a nucleophile (Table 1, Entry 6). The stark contrast between the reactivity of C_6F_5Cl and that of 2-PyCl can hardly be solely explained on the basis of the difference between their reduction potentials, which are quite close (vide supra). In other words, one cannot expect that C_6F_5Cl behaves exclusively as a classic sacrificial oxidant while 2-PyCl would act as a more efficient coupling partner.

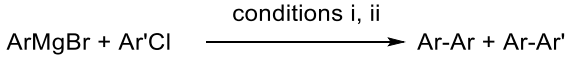

Entry	Ar	Ar-Ar	Ar-Ar'	Ar-Ar	Ar-Ar'
		Ar' = C_6F_5 ; conditions i : C_6F_5Cl, ArMgBr 1 M (1.2 equiv.), $FeCl_3$ 3 mol%, THF, 20°C, 4h		Ar' = 2-Py ; conditions ii : 2-PyCl, ArMgBr 1 M (1.2 equiv.), $Fe(acac)_3$ 5 mol%, THF, 0°C, 3h	
1	Ph	87 (**1a**) 85[a] (**1a**)	traces traces	26 (**1a**) n.d.	8 (**1b**) 9[b] (**1b**)
2	*p*-Me-C_6H_4	94 (**2a**)	traces	29 (**2a**)	13 (**2b**)
3	*m*-Me-C_6H_4	-	-	28 (**3a**)	11 (**3b**)
4	*p*-MeO-C_6H_4	88 (**4a**)	traces	32 (**4a**)	16 (**4b**)

5	*o*-MeO-C_6H_4	75 (**5a**)	traces	-	-
6	*p*-Me_2N-C_6H_4	85 (**6a**)	traces	22 (**6a**)	22 (**6b**)
7	*p*-CF_3-C_6H_4	-	-	48 (**7a**)	traces
8	*p*-F-C_6H_4	-	-	22 (**8a**)	3 (**8b**)
9	2-mesityl	20 (**9a**)	traces	-	-
10	1-naphthyl	70 (**10a**)	traces	-	-
11	2-naphthyl	90 (**11a**)	traces	-	-

Table 1: iron-catalyzed coupling of aryl Grignard reagents with C_6F_5Cl or 2-PyCl (isolated yields; non-isolated products were detected as minor peaks by GC-MS analysis (< 5%)); a) conditions ii were used; b) in the presence of 5 equiv. TEMPO per mole of iron.

In contrast with its reduction potential which should allow an activation by single-electron transfer (E_{red} = -2.05 V *vs* SCE), C_6F_5Cl did not led to the formation of detectable quantities of homocoupling product C_6F_5-C_6F_5 arising from the recombination of $C_6F_5^{\bullet}$ radicals. This behavior is in stark contrast with what was reported for an important number of cross-couplings involving other aryl halides, which proved to undergo a SET step to afford the corresponding radical R'$^{\bullet}$ followed by dimerization of the latter.[22] Noteworthy, activation of organic halides by a SET (followed by homodimerization of the corresponding radical) promoted by iron complexes under reducing conditions is also widely described when aliphatic electrophiles are used. Alkyl radicals are indeed more easily formed than their sp2 analogues, due to the weaker bond dissociation energy of the former.[29] It was for example demonstrated that 1,2-dichloroisobutane (DCIB) acted as a one-electron sacrificial oxidant in Nakamura's Fe-mediated C-H functionalization systems within a Fe^{II} / Fe^{III} / Fe^{I} two-step redox sequence. In that case, the key formation of cross-coupled product is allowed by monoelectronic oxidation of a transient bis-hydrocarbyliron(II) intermediate to the Fe^{III} stage, a fast reductive elimination occurring in the latter. A Fe^{I} species is finally obtained, again oxidized by DCIB in a one-electron process.[30-31] A similar Fe^{II} / Fe^{III} / Fe^{I} sequence has been reported by Deng for a bis-phenyl Fe^{II} complex stabilized by N-Heterocyclic Carbenes (NHCs), $(IPr_2Me_2)_2Fe^{II}(Ph)_2$, which generates the corresponding bisaryl Ph-Ph upon single-electron oxidation

by a ferrocenium salt followed by a 2-electron reductive elimination. In that case, the corresponding Fe^{I} complex is trapped *in situ* by PMe_3 to afford the 15-electron adduct $[(IPr_2Me_2)_2Fe^{I}(PMe_3)_2]^{+}$.[32]

In the system discussed herein though, no monoelectronic oxidation of *ate* $[Ar_3Fe^{II}]^{-}$ intermediates by C_6F_5Cl occurs to induce formation of Ar-Ar by a subsequent Fe^{III}-to-Fe^{I} reductive elimination, as attested by our previous studies (Ar = Mes).[23] From a mechanistic standpoint, it is known that Fe^{II} or Fe^{III} precursors such as $FeCl_n$ (n = 2, 3) or $Fe(acac)_3$ quickly afford *ate* ferrous species such as $[Ar_3Fe^{II}]^{-}$ in the presence of an excess of ArMgBr (Ar = Ph,[28,33], Mes[10]). Those complexes then evolve in the absence of a stabilizing co-ligand to lower Fe^{0} and Fe^{I} oxidation states, the zerovalent Fe^{0} species being predominant (ca. 85% of the iron distribution),[27] and transiently stabilized by arene ligation with suitable species (toluene co-solvent, or biphenyl formed by oxidation of PhMgBr). This arene-stabilized complex $(\eta^4\text{-arene})_2Fe^{0}$ finally evolves to non-reactive aggregates. Amongst this distribution of Fe^{II}, Fe^{I} and Fe^{0} intermediates obtained in the reaction medium, we recently demonstrated that the more reduced one was the only active species towards the C_6F_5Cl or 2-PyCl electrophiles (Scheme 3).

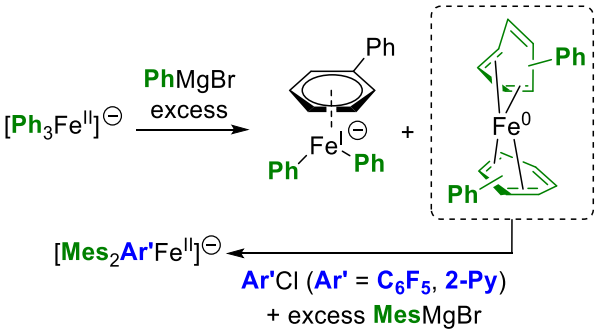

Scheme 3 : evolution of transient *ate*-Fe^{II} complexes towards Fe^{0} and Fe^{I} intermediates; the Fe^{0} promotes the 2-electron activation of electron-poor electrophiles (C_6F_5Cl or 2-PyCl).

This led to the observation of heteroleptic adducts $[Ar_2Ar'Fe^{II}]^{-}$ (Ar = Mes, Ar' = C_6F_5 or 2-Py) by ^{1}H and ^{19}F paramagnetic NMR, those complexes being formed by a 2-electron oxidative addition between Fe^{0} and the electrophilic partner Ar'X.[23] In line with the occurrence of this bielectronic activation, the yield of the cross-coupling between PhMgBr and 2-PyCl is not affected by the presence of a radical scavenger (TEMPO herein, see Table 1, Entry 1), suggesting that the coupling mechanism does not rely on monoelectronic steps. Therefore,

the formation of the Fe^0 oxidation state is crucial to the proficiency of the 2-electron oxidative addition allowing the activation of Ar'X. Thus, we first confirmed that *in situ* reduction of classic iron precursors ($FeCl_3$, $FeCl_2$) by a variety of aromatic Grignard reagents occurred efficiently. As shown below (Table 2), the addition of an excess (10 equivalents) of various aryl magnesium bromides (substituted by either electron-donating (Entries 2-3) or electron-withdrawing groups (Entry 4)) to a solution of $FeCl_3$ in THF leads to 1.4 to 1.6 equivalents of biaryl with a short 5 min reaction time. This is consistent with the average reduction of Fe^{III} to the Fe^0 stage, with an overall transfer of 3 electrons per mole of starting iron precursor. In a similar way, $FeCl_2$ (associated or not to LiCl to circumvent solubility issues) is reduced to Fe^0 oxidation state, showing that formation of the latter can be achieved in those conditions regardless of the electronic properties of the aryl Grignard reagent. Some of us demonstrated that reduction of $FeCl_3$ or $Fe(acac)_3$ by an excess of PhMgBr also afforded a minor *ate*-Fe^I complex (ca. 10-15% of the overall iron quantity), $[(\eta^6\text{-arene})Fe^I(Ph)_2]^-$ (arene = toluene when used as a co-solvent,[27] or Ph-Ph formed by oxidation of the nucleophile[34]). Analysis of the reaction medium by X-band EPR spectroscopy also revealed that reduction of $Fe(acac)_3$ by several aryl Grignard reagents (ArMgBr) in conditions of Table 2 also afforded similar low-spin Fe^I intermediates at low concentrations ($S = 1/2$, see Figure 1a for Ar = Ph (g = 2.206; 2.021; 1.999) and SI for Ar =*p*-MeO-C_6H_4 and *p*-F-C_6H_4). Fe^I oxidation state indeed represents ca. 5.4% of the overall iron quantity after reduction of $Fe(acac)_3$ by PhMgBr, and 9.6% when *p*-F-C_6H_4MgBr is used. Traces of Fe^I species (0.2% of the iron quantity) are detected upon reduction by *p*-MeO-C_6H_4MgBr. In all cases, formation of the homocoupling bisaryl product Ar-Ar as well as of the Fe^0 oxidation state as a major product upon reduction of the iron precursor by the aryl Grignard reagent ensures a first catalyst turnover in the homocoupling process.

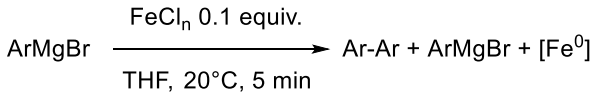

Entry	ArMgBr	ArAr *vs* Fe		% [Fe^I] (*vs* total [Fe])
		$FeCl_3$	$FeCl_2$	
1	PhMgBr	1.4 equiv (**1a**)	1.1 equiv (**1a**)	5.4
2	*p*-Me-C_6H_4MgBr	1.5 equiv (**2a**)	1 equiv[a] (**2a**)	n.d.
3	*p*-MeO-C_6H_4MgBr	1.4 equiv (**4a**)	-	0.2
4	*p*-F-C_6H_4MgBr	1.6 equiv (**8a**)	-	9.6

Table 2 : reduction of iron salts $FeCl_n$ (n = 2 or 3) by several aryl Grignard reagents leading to the corresponding bisaryls; reactions performed on a 13 mmol scale; a) the same result was obtained from $FeCl_2$•2 LiCl; speciation of low-spin EPR-active Fe^I formed upon reduction of $Fe(acac)_3$ by several Grignard reagents (15 equiv. *vs* Fe).

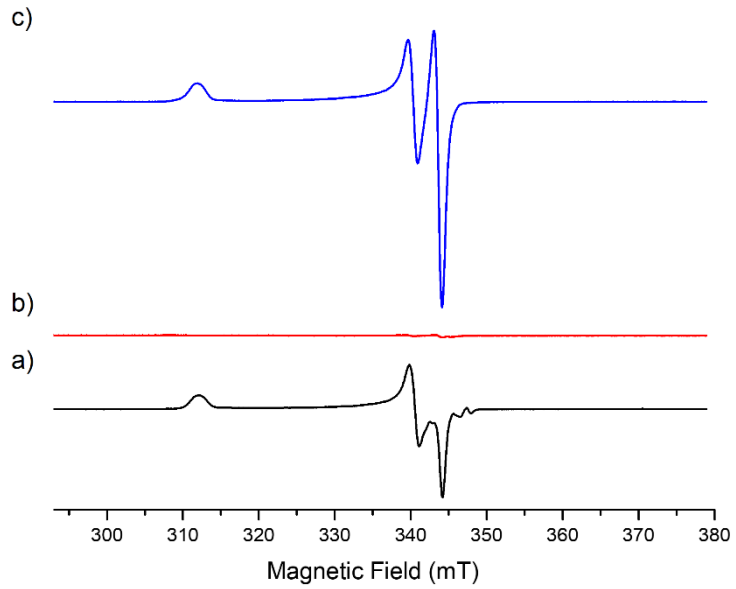

Figure 1 : X-band EPR analysis (T = 90 K) of a solution of a) $Fe(acac)_3$ (9 mM in a 98:2 THF:2-MeTHF mixture) treated by 15 equiv. PhMgBr; b), c): the same, after addition of resp. C_6F_5Cl or 2-PyCl (10 equiv. *vs* Fe); samples frozen after a 10 min reaction time at room temperature.

Reactivity of the minor Fe^I oxidation state towards C_6F_5Cl and 2-PyCl has also been monitored by EPR spectroscopy (Figure 1b,c). As discussed above, reduction of a solution of $Fe(acac)_3$ by 15 equiv. PhMgBr affords 5.4% of $[(\eta^6\text{-PhPh})Fe^I(Ph)_2]^-$ (*vs* total iron concentration). Addition of 10 equiv. C_6F_5Cl on this solution led to the disparition of the Fe^I signal (Figure 1b), suggesting a possible electron transfer between those two

species. It is however difficult to delineate the nature of the organic products formed by reaction of [(η^6-PhPh)$Fe^I(Ph)_2$]$^-$ with C_6F_5Cl, since the former complex only represents a small quantity of the overall iron distribution. However, the genuine reactivity of [(η^6-PhPh)$Fe^I(Ph)_2$]$^-$ towards a variety of organic halides has already been described by Hu[34] who reported that it mostly led to the homocoupling Ph-Ph product along with small amounts of cross-coupling. On the other hand, the Fe^I oxidation state is not affected by the addition of 10 equiv. 2-PyCl, attesting to the absence of electron transfer between those two species. This result is in line with the respective reduction potentials of C_6F_5Cl and 2-PyCl, the latter being less easily reduced. A slight alteration of the symmetry of the Fe^I signal is observed (Figure 1c), which might be due to the formation of a new species involving 2-PyCl as a ligand to the Fe^I ion. Similar trends are observed regarding the reactivity of the Fe^I species generated by reduction of $Fe(acac)_3$ with *p*-F-C_6H_4MgBr towards C_6F_5Cl and 2-PyCl (see Figure S3). The evolution of the distribution of Fe^I species formed by reduction of $Fe(acac)_3$ with *p*-MeO-C_6H_4MgBr after reaction with 2-PyCl is more unclear (Figure S4), but this oxidation state does not represent more than 1.5% of the overall iron quantity. In the next section, the productive pathways followed in the cross- and homo-coupling reactions involving the major Fe^0 species obtained by reduction of the iron precursor are discussed.

Fate of the C_6F_5 and 2-Py groups in the catalytic process. Since only traces of cross-coupling products Ar-C_6F_5 are detected (Table 1) in spite of the evidence of the formation of C_6F_5-[Fe^{II}] species upon activation of the C_6F_5-Cl bond, the fate of the C_6F_5 group in the overall process was then investigated. When *p*-MeO-C_6H_4MgBr and C_6F_5Cl (in a 1:0.55 ratio) were used as coupling reagents, an electrophilic quench of the medium by octanoic anhydride shows a very good 88% formation yield of the expected (4,4')-bisanisyl homocoupling product **4a**, along with 55% of ketone *n*-$C_7H_{15}C(O)C_6F_5$ (**12**, Scheme 4). In other words, the C_6F_5 group is catalytically released in the reaction medium as its 2-electron reduced anion $C_6F_5^-$ - the presence of Mg^{II} cations moreover probably triggers the transfer of the $C_6F_5^-$ anion from the iron center to afford the corresponding Grignard, C_6F_5MgBr. The later is afterwards quantitatively trapped by electrophilic quenching using octanoic anhydride.[35]

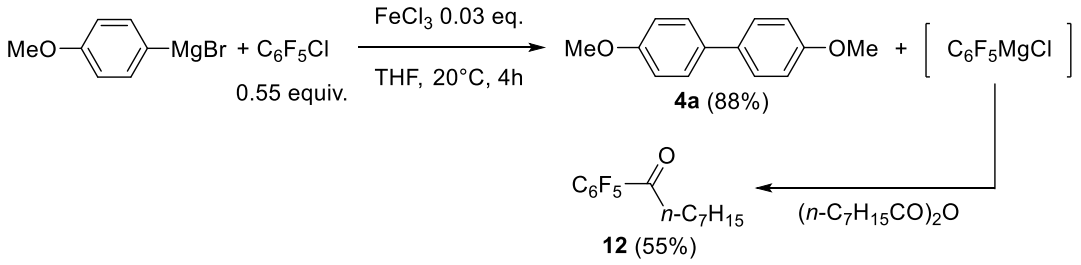

Scheme 4 : electrophilic quench of the $C_6F_5^-$ anion after its release in the reaction medium.

The quantitative electrophilic quenching of the $C_6F_5^-$ anion at the end of the attempt of cross-coupling between *p*-MeO-C_6H_4MgBr and C_6F_5Cl suggests that the Fe^{II}-ligated $C_6F_5^-$ anion formed by oxidative addition of Fe^0 onto C_6F_5Cl is unreactive in the coupling catalytic process. The intrinsic stability of the C_6F_5-[Fe^{II}] bond has also been investigated by transmetallation of C_6F_5MgBr with an Fe^{II} precursor. Reaction of 2 equiv. C_6F_5MgBr with $FeCl_2$ led to the formation of a new organoiron(II) intermediate, characterized by a paramagnetic resonance at 283 ppm in ^{19}F NMR (Figure 2a), attesting to the transmetallation of a $C_6F_5^-$ anion with a paramagnetic center. Further addition of an excess of MesMgBr (20 equiv. *vs* Fe) after 3 hours at 20°C led to the sole observation of $[Mes_3Fe^{II}]^-$ species in ^{1}H NMR (characterized by two sharp downfielded peaks at 112 and 127 ppm in a 3:2 ratio, Figure 2b[10]) and to a ^{19}F-NMR silent spectrum. This shows that $[Mes_3Fe^{II}]^-$ was formed by substitution of the Fe^{II}-ligated $C_6F_5^-$ anions by their mesityl analogues. More importantly, this demonstrates that addition of C_6F_5MgBr onto a Fe^{II} salt did not lead to the reduction of the ferrous ion, suggesting that the C_6F_5-[Fe^{II}] bond displays to a certain extent an appreciable thermal stability.

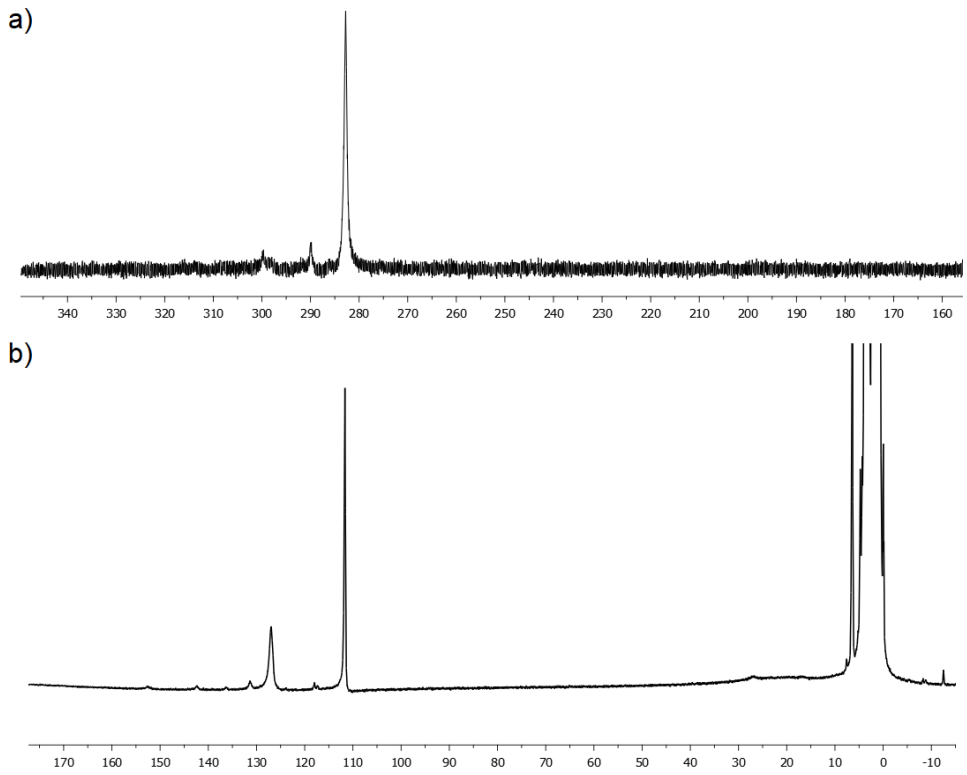

Figure 2: a) ^{19}F NMR spectrum (377 MHz, THF d_8) of a solution of $FeCl_2$ treated by 2 equiv. C_6F_5MgBr; b) ^{1}H NMR spectrum (400 MHz) recorded 3h after addition of 20 equiv. MesMgBr at 20°C.

The intermediate C_6F_5-[Fe^{II}] adduct generated by transmetallation of C_6F_5MgBr onto $FeCl_2$ also proved to be stable at -10 °C up to 15h, since 88% of C_6F_5I is obtained by iodometric titration under those conditions. This stability is in stark contrast with other well-known Ar-[Fe^{II}] species (such as [Ph_3Fe^{II}]$^{-}$), which readily undergo decomposition towards lower Fe^0 or Fe^I oxidation states along with either arenes Ar-H or bisaryls Ar-Ar by reductive elimination.[28] Evolution of the C_6F_5-[Fe^{II}] adduct at 30°C has further been monitored by iodolysis (Table 3). It is interesting to note that the decomposition of the latter occurs slowly at this temperature, and mainly gives C_6F_5H as a reduction byproduct, rather than the bisaryl C_6F_5-C_6F_5.

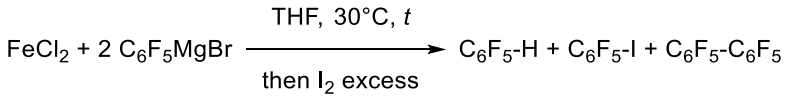

Time (h)	C_6F_5H (%)	C_6F_5I (%)	C_6F_5-C_6F_5 (%)
0.25	38	47	7
3	42	38	10
24	52	21	14
90	59	3	19

Table 3: GC-monitoring (internal standard : undecane) of the decomposition product formed after transmetallation of C_6F_5MgBr (2 equiv.) onto $FeCl_2$ in THF at 30°C, after iodolysis quench.

Those results overall demonstrate a reactivity of the C_6F_5-[Fe^{II}] bond significantly lower than that of a classic Ar-[Fe^{II}] compound, which usually follows much faster reductive pathways. A weak nucleophilicity is also observed for those C_6F_5-[Fe^{II}] adducts. Indeed, Mg-to-Fe transmetallation of C_6F_5MgCl onto $FeCl_2$ (two equiv. per mole of iron) also results in the absence of detection of ketone $C_6F_5C(O)(n\text{-}C_7H_{15})$ (**12**) upon electrophilic quenching of the reaction medium by ester $n\text{-}C_7H_{15}C(O)Et$, whereas treatment of C_6F_5MgCl by this ester quantitatively affords the expected ketone **12** along with the tertiary alcohol $(C_6F_5)_2C(OH)(n\text{-}C_7H_{15})$ in a global 92% yield. The C_6F_5-[Fe^{II}] bond thus shows a decreased nucleophilic reactivity compared to C_6F_5MgCl. In line with its greater reactivity as a cross-coupling partner, 2-PyCl only affords traces (<5%) of 2-PyI upon iodolysis quench of a coupling medium (see conditions in Table 1, Entry 1). In other words, a much smaller quantity of the 2-Py^- anion is released in the reaction medium compared to that of $C_6F_5^-$ anion. In order to rationalize the mechanistic facets of the cross- versus homocoupling competition in those 2-electron processes as well as the striking differences displayed by C_6F_5Cl and 2-PyCl, the evolution of the $[Ar_2Ar'Fe^{II}]^-$ intermediate (Ar' = C_6F_5 or 2-Py) in the catalytic medium was then investigated more precisely.

Key 2-electron reductive elimination in cross- and homocoupling pathways. Heteroleptic species $[Ar_2Ar'Fe^{II}]^-$ is formed by oxidative addition of a Fe^0 intermediate onto Ar'Cl (Ar' = C_6F_5 or 2-Py) in the presence of ArMgBr at early stages of the catalytic process (Scheme 3). This complex is likely involved as a key intermediate in both cross-coupling and homocoupling pathways through 2-electron reductive elimination

steps, as detailed in Scheme 5. Tris-coordinated (*t*) $[Ar_2Ar'Fe^{II}]^-$ can indeed evolve towards the formation of either the cross-coupling Ar-Ar' (path i) or homocoupling Ar-Ar (path ii) products. Alternatively, $[Ar_2Ar'Fe^{II}]^-$ can undergo an additional transmetallation with an equivalent of ArMgBr[28] leading to quaternized *ate*-Fe^{II} species (*q*) such as $[Ar_3Ar'Fe^{II}Mg(THF)])$. Formation of quaternized adducts involving an *ipso* coordination of a Li^+ cation were also reported earlier by Fürstner and structurally characterized.[36] Such quaternized intermediates can also provide both cross-coupling or homocoupling products (following respectively paths iii and iv). $[Ar_3Ar'Fe^{II}Mg(THF)]$ can also release one equivalent of Ar'MgBr, leading to the homoleptic species $[Ar_3Fe^{II}]^-$, which is solely able to afford the homocoupling product Ar-Ar by reductive elimination (path v).

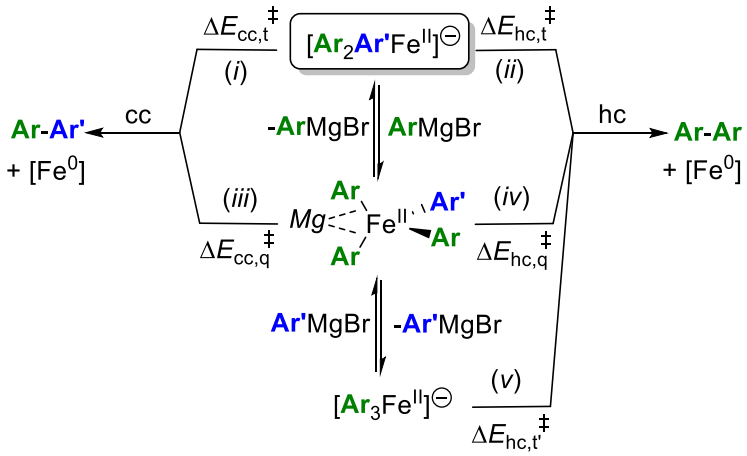

Scheme 5: formation of cross-coupling (cc) and homocoupling (hc) products by 2-electron reductive elimination occurring in heteroleptic $[Ar_2Ar'Fe^{II}]^-$ and $[Ar_3Ar'Fe^{II}Mg(THF)]$, and in homoleptic $[Ar_3Fe^{II}]^-$ complexes; *Mg* = $Mg(THF)^{2+}$.

Intermediates $[Ar_2Ar'Fe^{II}]^-$, $[Ar_3Ar'Fe^{II}Mg(THF)]$ and $[Ar_3Fe^{II}]^-$ being accessible in usual coupling conditions,[23,28] the feasibility of the reaction paths i-v was then investigated by DFT calculations (Ar = Ph and Ar' = C_6F_5 or 2-Py). The corresponding computed activation energies are reported in Table 4. OPBE functional was used, associated to the following basis sets: 6-31+G* (C, H, O, N, Mg, F, Br), SDD and pseudo-potential (Fe). Solvent (THF herein) was described using the PCM model. Similar trends were obtained using the more computationally costly Ahlrich's basis set and pseudo-potential def2TZVPP for Fe (see Table S1). In those calculations, the *tris* coordinated *ate* species $[Ar_2Ar'Fe^{II}]^-$ and $[Ar_3Fe^{II}]^-$ have been computed using a high-

spin (S = 2) ground multiplicity, whereas the other structures (including the reductive elimination transition states for paths i-v) have been computed on the triplet spin surface (S =1). Those choices have been motivated by previous reported results showing that those were the ground spin multiplicities of the analogous paths involving $[Ph_3Fe^{II}]^-$ and $[Ph_4Fe^{II}MgBr(THF)]^-$ species (see SI for the computational details and for full calculated surfaces of paths i and ii with Ar'= 2-Py).[28]

	Path i	Path ii	Path iii	Path iv	Path v
	$\Delta E_{cc,t}^{\ddagger}$	$\Delta E_{hc,t}^{\ddagger}$	$\Delta E_{cc,q}^{\ddagger}$	$\Delta E_{hc,q}^{\ddagger}$	$\Delta E_{hc,t'}^{\ddagger}$
Ar = Ph Ar' = C_6F_5	28.5	16.7	18.3	11.9	17.0
Ar = Ph Ar' = 2-Py	12.5	16.9	10.6	4.6	

Table 4: thermal activation energies of the cross- and homocoupling paths discussed in Scheme 5; energies given in kcal.mol^{-1} with respect to $[Ar_2Ar'Fe^{II}]^-$ (paths i,ii), $[Ar_3Ar'Fe^{II}Mg(THF)]$ (paths iii, iv), or $[Ar_3Fe^{II}]^-$ (path v); *Mg* = $Mg(THF)^{2+}$.

In all cases, formation of the homocoupling product (PhPh) is favored when C_6F_5Cl is used as an electrophile. Regardless of the nature of the heteroleptic intermediate ($[Ph_2(C_6F_5)Fe^{II}]^-$, or $[Ph_3(C_6F_5)Fe^{II}Mg(THF)]$), the activation energy of the cross-coupling (paths i or iii) is indeed much higher than that of the homocoupling (paths ii and iv). This is in line with the experimental results reported in Table 1, showing that only traces of cross-coupling products Ar-C_6F_5 are formed in such conditions. It is interesting to notice that the transition states computed on the cross-coupling surfaces for the formation of Ph-C_6F_5 by reductive elimination (paths i and iii) differ from the classic 3-center synchronous structure. Those transition states are more accurately described by the iron-to-carbon migration of the electron-rich phenyl anion onto the electron poor Fe^{II}-ligated C_6F_5 group. This mechanism is much similar to the first step of a S_NAr process, involving the formation of a dearomatized Meisenheimer intermediate (Scheme 6a, top). This is attested in the computed structure of those transition states by a strong pyramidalization of the C atom in the *para* position of the C_6F_5 ring, with computed $C_{ipso}C_{para}F$ angles of resp. 166° and 167° in the *tris*- (path i) and *tetra*-coordinated (path iii) structures (Schemes 6a, bottom, and 6b). Accordingly, a negative charge develops at the C_{para} atom within this migration: the computed Mulliken

charge for example decreases from 0.1 |e| in $[Ph_2(C_6F_5)Fe^{II}]^-$ to -0.3 |e| in the corresponding transition state. A similar evolution is observed in the tetracoordinated series (evolution from a 0.0 |e| charge on the C_{para} atom of the C_6F_5 ring in $[Ph_3(C_6F_5)Fe^{II}Mg(THF)]$ to a more negative -0.2 |e| charge in the transition state).

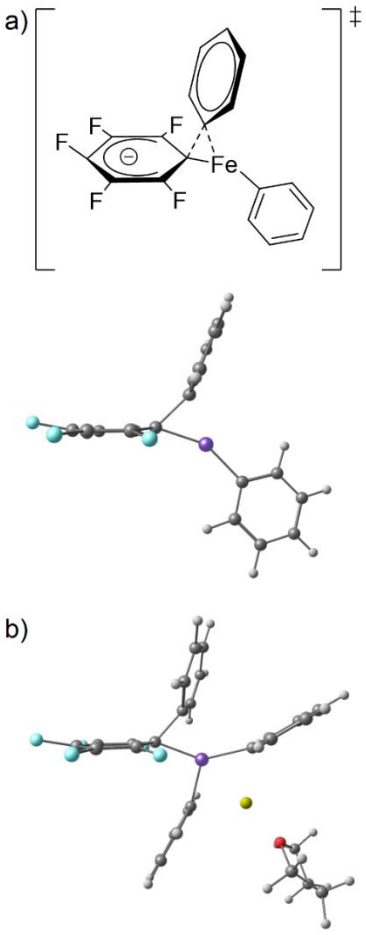

Scheme 6 : DFT-computed reductive elimination transition states of Ph-C_6F_5 from a) $[Ph_2(C_6F_5)Fe^{II}]^-$ and b) $[Ph_3(C_6F_5)Fe^{II}Mg(THF)]$ on the triplet (S = 1) surface.

The situation is quite different in the coupling series involving 2-PyCl. $[Ph_2(2\text{-}Py)Fe^{II}]^-$ indeed preferentially follows the cross-coupling path, whose activation energy is lower by 4.4 kcal.mol^{-1} with respect to that of the homocoupling (resp. path i and ii). Quaternized adduct $[Ph_3(2\text{-}Py)Fe^{II}Mg(THF)]$ evolves on the other hand more easily along the homocoupling path, akin to its C_6F_5-ligated analogue (comparison of paths iii and iv). The remarkably low activation barrier for the homocoupling path involving the quaternized species $[Ph_3(2\text{-}Py)Fe^{II}Mg(THF)]$ (4.6 kcal.mol^{-1}) is due to a N-ligation of the iron center in the transition state, which does not

occur in the cross-coupling reductive elimination (path iii: 10.6 kcal.mol^{-1}, Table 4). Since the sole intermediate allowing the formation of the cross-coupling product requires a low Ph:Fe transmetallation degree (Ph:Fe = 2 in $[Ph_2(2\text{-}Py)Fe^{II}]^-$, whereas Ph:Fe = 3 in $[Ph_3(2\text{-}Py)Fe^{II}Mg(THF)]$), this also explains why a slow addition of the Grignard reagent is crucial in those coupling systems. Indeed, a fast addition of this reagent would lead to an increased concentration of the quaternized species, which favors the formation of the homocoupled bisaryl (either directly (path iv) or after formation of the homoleptic species $[Ph_3Fe^{II}]^-$ (path v)).

The reductive elimination of Ph-Ph from a *tris*-coordinated species moreover does not seem to be affected by the nature of the third ligand, since the computed activation energy is quite the same (ca. 17 kcal.mol^{-1}, paths ii and v, Table 4) starting from either $[Ph_2(C_6F_5)Fe^{II}]^-$, $[Ph_2(2\text{-}Py)Fe^{II}]^-$, or $[Ph_3Fe^{II}]^-$. Conversely, reductive elimination of the Ph-Ar' cross-coupling product is strongly affected by the electronic properties of the Ar' ring since it evolves from 12.5 kcal.mol^{-1} (Ar' = 2-Py) to 28.5 kcal.mol^{-1} (Ar' = C_6F_5) (Table 4). Similar observations can be made for the quaternized species $[Ph_3(Ar')Fe^{II}Mg(THF)]$ (Ar' = C_6F_5, 2-Py). When the coupling mechanism is dominated by 2-electron processes, the reductive elimination leading to the cross-coupling product starting from heteroleptic species $[Ar_2Ar'Fe^{II}]^-$ involves a migration of the electron-rich Ar group onto the electron-poor Ar' moiety (the former being derived from the nucleophile ArMgBr, the later from the electrophile Ar'Cl), as shown in Scheme 6a. Existence of an energetically accessible antibonding π* system borne by the Fe^{II}-ligated Ar'^- ligand is thus a first prerequisite to ensure the initiation of the reductive elimination on the cross-coupling path. Owing to their electron-poor character, both C_6F_5 and 2-Py rings fulfill this condition in the present study. However, completion of the reductive elimination process also requests in a second time an efficient transfer of the two electrons located onto the Ar' ring in the transition state onto the Fe^{II} ion, allowing its reduction to the Fe^0 stage. This requires a sufficient reductive power of the Ar'-$[Fe^{II}]$ σ bond. Therefore, although the electron-poor character of the Ar' group enables the transfer of the Ar ring thanks to an accessible π* system, it also translates into a decreased reducing power of the Ar'-$[Fe^{II}]$ σ bond. The balance between these two opposite electronic requirements thus governs the strong discrepancy observed between C_6F_5Cl and 2-PyCl. The former is far too electron-poor to afford a reductive C_6F_5-$[Fe^{II}]$ intermediate: no cross-coupling product is observed, and only byproducts derived from anion $C_6F_5^-$ are detected (C_6F_5H,

C_6F_5-C_6F_5). On the other hand, 2-PyCl reaches a good compromise between its π-accepting effects and σ-donating properties of the 2-Py-[Fe^{II}] bond, overall allowing its use as a cross-coupling partner.

In the last section, the role of the electronic properties of the Ar ligand in the cross- versus homocoupling competition has been investigated more closely.

Electronic effects at play in the cross- versus homocoupling competition. Analysis of the cross-coupling (cc) *versus* homocoupling (hc) ratio depending on the electronic effects of the substituents borne by the Grignard reagent ArMgBr was performed using 2-PyCl as an electrophile (see Table 1). The cross-coupling ratio r_{cc} (r_{cc} = [cc]/([cc]+[hc])) was found to decrease with the value of the σ Hammett parameter of the nucleophilic partner, as shown in Figure 3a. This demonstrates that the cross-coupling pathway is more easily followed when electron-rich nucleophiles are used, r_{cc} being higher for negative σ parameters (a maximum value of r_{cc} = 0.5 is obtained when *p*-Me_2N-C_6H_4MgBr is used).

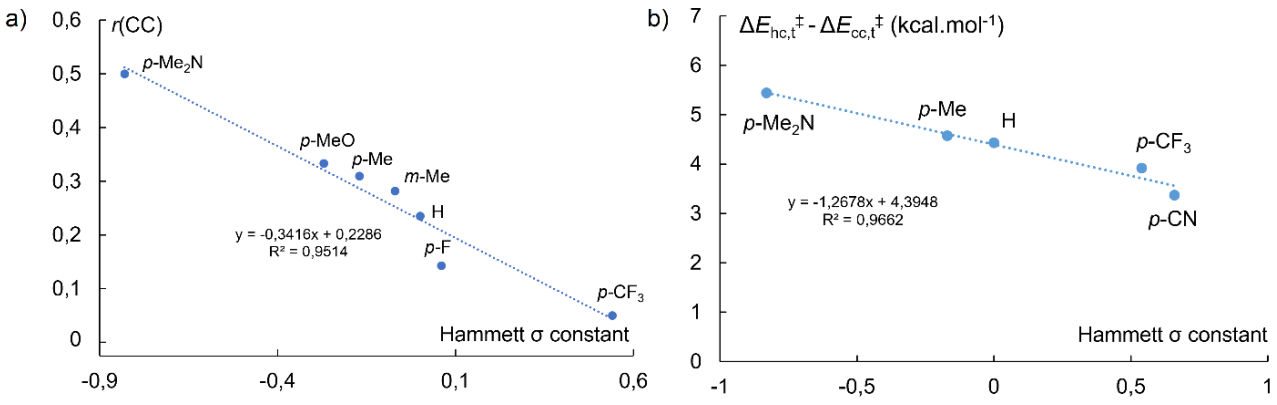

Figure 3 : a) experimental evolution of the cross-coupling (cc) *versus* homocoupling (hc) ratio r_{cc} for ArMgBr / 2-PyCl coupling systems reported in Table 1; b) DFT-computed evolution of the activation free energy gap between the cross- and homocoupling paths undergone by [Ar_2(2-Py)Fe^{II}]$^-$ intermediates.

This tendency has also been reproduced *in silico* (Figure 3b). DFT calculations indeed show that the gap between the computed free energy activations of the homo- and the cross-coupling paths involving *ate* [$Ar_2Ar'Fe^{II}$]$^-$ species (paths i and ii in Scheme 5) increases when the Ar^- anion is substituted with electron-

donating substituents. Those results are consistent with the 2-electron reductive elimination mechanism discussed above for Ar-C_6F_5 coupling products, with a key migration of the electron-rich Ar anion onto the electron-poor Ar' ring: the electron-richer the Ar anion, the more efficient the migration. Overall, this also explains why the best match leading to a good cross-coupling *versus* homocoupling ratio in the aryl-heteroaryl series is obtained, for a given electrophile, using electron-rich nucleophiles.

In addition to the role played by the electronic effect of the substituents borne by the nucleophile on the kinetics trends of the reductive elimination, the nature of the nucleophile may also affect the preferred pathway (cross-coupling or homocoupling) at an earlier stage of the catalysis. Previous DFT calculations indeed suggested that the stable resting state of the Fe^0 species generated *in situ* by reduction of the iron precursor (Scheme 7) may involve an aryl anion σ-bonded to the Fe^0, by transmetallation of ArMgBr with the complex $(\eta^4\text{-arene})_2Fe^0$.[23]

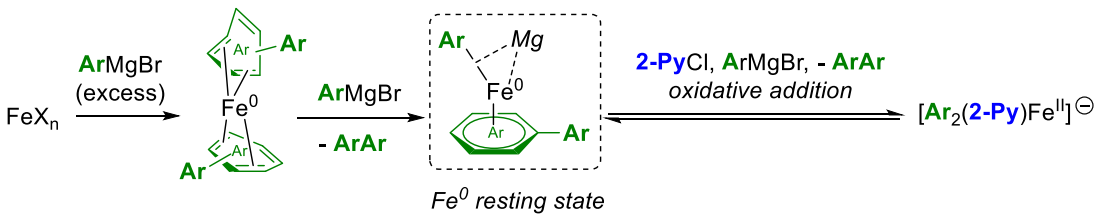

Scheme 7 : formation of a Fe^0 resting state σ-coordinated by an Ar^- anion leading to $[Ar_2(2\text{-Py})Fe^{II}]^-$ after oxidative addition with 2-PyCl ; *Mg* = $MgBr(THF)^+$ (model structures investigated by DFT calculations).

Therefore, when electron-rich Grignard reagents ArMgBr are used as nucleophilic partners, the Fe^0 resting state $(\eta^6\text{-ArAr})Fe^0(ArMgBr(THF))$ displays an enhanced reducing power. Due to the electron richness of the iron center, a faster oxidative addition of intermediate Ar-[Fe^0] onto 2-PyCl should occur, then leading to a higher dynamic concentration of the $[Ar_2(2\text{-Py})Fe^{II}]^-$ species and thus to a lower ArMgBr : $[Ar_2(2\text{-Py})Fe^{II}]^-$ ratio. Consequently, this also would slightly inhibit the quaternization process and therefore decrease the formation of the bisaryl Ar-Ar, given that the quaternized species selectively affords the homocoupling product (see paths iii and iv, Scheme 5, and Table 4).

CONCLUSION

Mechanistic patterns involved in iron-mediated cross-couplings are highly complex, since the nature of the active species and of the elementary steps are strongly dependent on the coupling partners physical properties (hybridization, oxidoreduction potentials, …). Therefore, generalities are difficultly drawn from mechanistic studies carried out on specific substrates since no universal mechanism can describe this variety of transformations. When 2-electron processes dominate the catalytic activity in aryl-(hetero)aryl couplings between ArMgBr nucleophiles and electron-poor Ar'Cl electrophiles, an heteroleptic complex $[Ar_2Ar'Fe^{II}]^-$ can be formed by oxidative addition of an Fe^0 species onto the Ar'-Cl bond. This *ate*-complex is a key intermediate, which can evolve by 2-electron reductive elimination along both cross- and homocoupling paths (directly or with the involvement of quaternized species such as $[Ar_3(Ar')Fe^{II}Mg(THF)]$). Such a bielectronic pattern is observed for example with Ar'-X substrates bearing an electron-poor Ar' ring and a difficultly reduced Ar'-X bond (typically with X = Cl). Combination of those two electronic effects allows the 2-electron mechanism to overcome the more usual monoelectronic reduction of the electrophilic partner in classic Kharasch-type Grignard oxidative homocouplings. Owing to an asynchronous reductive elimination mechanism involving a migration of the Ar^- anion onto the Ar' ring, the cross-coupling path is more favored compared to the homocoupling when electron-rich Ar nucleophiles are used. Those results also demonstrate that the competition between aryl-aryl cross-coupling and nucleophile oxidative homocoupling cannot be rationalized solely on the basis of the reduction potential of the electrophilic partner when the reactivity of the system is driven by 2-electron elementary steps.

REFERENCES

[1] Tamura, M.; Kochi, J. K. Vinylation of Grignard reagents. Catalysis by iron. *J. Am. Chem. Soc.* **1971**, *93*, 1487–1489.

[2] Neumann, S. M.; Kochi, J. K. Synthesis of olefins. Cross-coupling of alkenyl halides and Grignard reagents catalyzed by iron complexes. *J. Org. Chem.* **1975**, *40*, 599–606.

[3] Cahiez, G.; Avedissian, H. Highly Stereo- and Chemoselective Iron-Catalyzed Alkenylation of Organomagnesium Compounds. *Synthesis* **1998**, *1998*, 1199–1205.

[4] Fürstner, A.; Leitner, A.; Méndez, M.; Krause, H. Iron-Catalyzed Cross-Coupling Reactions. *J. Am. Chem. Soc.* **2002**, *124*, 13856–13863.

[5] Martin, R.; Fürstner, A. Cross-Coupling of Alkyl Halides with Aryl Grignard Reagents Catalyzed by a Low-Valent Iron Complex. *Angewandte Chemie International Edition* **2004**, *43*, 3955–3957.

[6] Nakamura, M.; Matsuo, K.; Ito, S.; Nakamura, E. Iron-Catalyzed Cross-Coupling of Primary and Secondary Alkyl Halides with Aryl Grignard Reagents. *J. Am. Chem. Soc.* **2004**, *126*, 3686–3687.

[7] Hatakeyama, T.; Hashimoto, T.; Kondo, Y.; Fujiwara, Y.; Seike, H.; Takaya, H.; Tamada, Y.; Ono, T.; Nakamura, M. Iron-Catalyzed Suzuki−Miyaura Coupling of Alkyl Halides. *J. Am. Chem. Soc.* **2010**, *132*, 10674–10676.

[8] Bedford, R. B.; Betham, M.; Bruce, D. W.; Danopoulos, A. A.; Frost, R. M.; Hird, M. Iron-phosphine, -phosphite, -arsine, and -carbene catalysts for the coupling of primary and secondary alkyl halides with aryl Grignard reagents. *J. Org. Chem.* **2006**, *71*, 1104-1110.

[9] Bedford, R. B.; Huwe, M.; Wilkinson, M. C. Iron-catalysed Negishi coupling of benzylhalides and phosphates. *Chem. Commun.* **2009**, *0*, 600–602.

[10] Bedford, R. B.; Brenner, P. B.; Carter, E.; Cogswell, P. M.; Haddow, M. F.; Harvey, J. N.; Murphy, D. M.; Nunn, J.; Woodall, C. H. TMEDA in Iron-Catalyzed Kumada Coupling: Amine Adduct versus Homoleptic "ate" Complex Formation. *Angew. Chem. Int. Ed.* **2014**, *53*, 1804–1808.

[11] R. B. Bedford, P. B. Brenner, The development of iron catalysts for cross-coupling reactions. Iron Catalysis II; Bauer, E., Ed.; Springer Intl., 2015; For complete reviews on Fe-catalyzed cross-couplings, see references [12], [13] and for a recent review on one-electron processes mediated by iron catalysts, see reference [14].

[12] Bauer, I.; Knölker, H.-J. Iron Catalysis in Organic Synthesis. *Chem. Rev*. **2015**, *115*, 3170–3387, section 2.4.1.

[13] Rana, S.; Biswas, J. P.; Paul, S.; Paik, A.; Maiti, D. Organic synthesis with the most abundant transition metal–iron: from rust to multitasking catalysts. *Chem. Soc. Rev.*, **2021**, 50, 243-472, section 6.

[14] Kyne, S. H.; Lefèvre, G.; Ollivier, C.; Petit, M.; Ramis Cladera, V.-A.; Fensterbank, L. Iron and cobalt catalysis: new perspectives in synthetic radical chemistry. *Chem. Soc. Rev*., **2020**, *49*, 8501-8542.

[15] Fürstner, A. Iron Catalysis in Organic Synthesis: A Critical Assessment of What It Takes To Make This Base Metal a Multitasking Champion. *ACS Cent. Sci*. **2016**, *2*, 778–789.

[16] Daifuku, S. L.; Kneebone, J. L.; Snyder, B. E. R.; Neidig, M. L. Iron(II) Active Species in Iron–Bisphosphine Catalyzed Kumada and Suzuki–Miyaura Cross-Couplings of Phenyl Nucleophiles and Secondary Alkyl Halides. *J. Am. Chem. Soc.* **2015**, *137*, 11432–11444.

[17] Carpenter, S. H.; Baker, T. M.; Muñoz III, S. B.; Brennessel, W. W.; Neidig, M. L. Multinuclear iron–phenyl species in reactions of simple iron salts with PhMgBr: identification of $Fe_4(\mu\text{-}Ph)_6(THF)_4$ as a key reactive species for cross-coupling catalysis. *Chem. Sci*., **2018**, *9*, 7931-7939.

[18] Kharasch, M. S.; Fields, E. K. Factors Determining the Course and Mechanisms of Grignard Reactions. IV. The Effect of Metallic Halides on the Reaction of Aryl Grignard Reagents and Organic Halides. *J. Am. Chem. Soc*. **1941**, *63*, 2316-2320.

[19] Sapountzis, I.; Lin, W.; Kofink, C. C.; Despotopoulou, C.; Knochel, P. Iron-Catalyzed Aryl–Aryl Cross-Couplings with Magnesium-Derived Copper Reagents. *Angew. Chem., Int. Ed*. **2005**, *44*, 1654-1657.

[20] Hatakeyama, T.; Nakamura, M. Iron-Catalyzed Selective Biaryl Coupling: Remarkable Suppression of Homocoupling by the Fluoride Anion. *J. Am. Chem. Soc.* **2007**, *129*, 9844–9845.

[21] Chua, Y.-Y.; Duong, H. A. Selective Kumada biaryl cross-coupling reaction enabled by an iron(iii) alkoxide–N-heterocyclic carbene catalyst system. *Chem. Commun.* **2014**, *50*, 8424–8427.

[22] Uchiyama, M.; Matsumoto, Y.; Nakamura, S.; Ohwada, T.; Kobayashi, N.; Yamashita, N.; Matsumiya, A.; Sakamoto, T. Development of a Catalytic Electron Transfer System Mediated by Transition Metal Ate Complexes: Applicability and Tunability of Electron-Releasing Potential for Organic Transformations. *J. Am. Chem. Soc*. **2004**, *126*, 8755–8759.

[23] Wowk, V.; Rousseau, L.; Lefèvre, G. Importance of Two-Electron Processes in Fe-Catalyzed Aryl-(hetero)aryl Cross-Couplings: Evidence of Fe^0/Fe^{II} Couple Implication. *Organometallics* **2021**, *40*, 19, 3253–3266.

[24] Muthukrishnan, A.; Sangaranarayanan, M. V. Mechanistic Analysis of the Reductive Cleavage of Carbon–Halogen Bonds in Halopentafluorobenzenes. *J. Electrochem. Soc*. **2009**, *156*, 23-28.

[25] Enemaerke, R. J.; Christensen, T. B.; Jensen, H.; Daasbjerg, K. Application of a New Kinetic Method in the Investigation of Cleavage Reactions of Haloaromatic Radical Anions. *J. Chem. Soc., Perkin Trans. 2* **2001**, 1620–1630.

[26] Cahiez, G.; Moyeux, A.; Buendia, J.; Duplais, C. Manganese- or Iron-Catalyzed Homocoupling of Grignard Reagents Using Atmospheric Oxygen as an Oxidant. *J. Am. Chem. Soc*. **2007**, *129*, *45*, 13788–13789.

[27] Clémancey, M.; Cantat, T.; Blondin, G.; Latour, J.-M.; Dorlet, P.; Lefèvre, G. Structural Insights into the Nature of Fe^0 and Fe^I Low-Valent Species Obtained upon the Reduction of Iron Salts by Aryl Grignard Reagents. *Inorg. Chem.* **2017**, *56*, 3834-3848.

[28] Rousseau, L.; Herrero, C.; Clémancey, M.; Imberdis, A.; Blondin, G.; Lefèvre, G. Evolution of Ate-Organoiron(II) Species towards Lower Oxidation States: Role of the Steric and Electronic Factors. *Chem. Eur. J.* **2020**, *26*, 2417-2428.

[29] This translates into lower bond dissociation energies of the C—X bonds in the aliphatic series. For instance, the C—I (resp. C—Br) bond at 298 K increases from 55.6 kcal.mol^{-1} in *t*Bu—I to 67 kcal.mol^{-1} in Ph—I (resp. from 72.6 kcal.mol^{-1} in *t*Bu—Br to 84 kcal.mol^{-1} in Ph—Br), see Blanksby, S. J.; Ellison, G. B. Bond Dissociation Energies of Organic Molecules. *Acc. Chem. Res.* **2003**, *36*, 255.

[30] Sun, Y.; Tang, H.; Chen, K.; Hu, L.; Yao, J.; Shaik, S.; Chen, H. Two-State Reactivity in Low-Valent Iron Mediated C-H Activation and the Implications for Other First-Row Transition Metals. *J. Am. Chem. Soc*. **2016**, *138*, 3715-3730.

[31] Boddie, T. E.; Carpenter, S. H.; Baker, T. M.; DeMuth, J. C.; Cera, G.; Brennessel, W. W.; Ackermann, L.; Neidig, M. L. Identification and Reactivity of Cyclometalated Iron(II) Intermediates in Triazole-Directed Iron-Catalyzed C–H Activation. *J. Am. Chem. Soc.* **2019**, *141*, 31, 12338–12345.

[32] Liu, Y.; Xiao, J.; Wang, L.; Song, Y.; Deng, L. Carbon–Carbon Bond Formation Reactivity of a Four-Coordinate NHC-Supported Iron(II) Phenyl Compound. *Organometallics* **2015**, *34*, 599-605.

[33] Rousseau, L.; Desaintjean, A.; Knochel, P.; Lefèvre, G. Iron-Catalyzed Cross-Coupling of Bis-(aryl)manganese Nucleophiles with Alkenyl Halides: Optimization and Mechanistic Investigations. *Molecules* **2020**, *25*, 723-734.

[34] Zhurkin, F.; Wodrich, M. D.; Hu, X. A Monometallic Iron(I) Organoferrate. *Organometallics* **2017**, *36*, 3, 499–501.

[35] Control experiments confirmed that pentafluorophenylmagnesium halide C_6F_5MgCl was not formed by direct magnesium-chloride exchange from ArMgBr and C_6F_5Cl. In the absence of catalyst, the exchange takes place with a low 3% yield.

[36] Fürstner, A.; Martin, R.; Krause, H.; Seidel, G.; Goddard, R., Lehmann, C. W. Preparation, Structure, and Reactivity of Nonstabilized Organoiron Compounds. Implications for Iron-Catalyzed Cross Coupling Reactions. *J. Am. Chem. Soc*. **2008**, *130*, 8773 – 8787.

ASSOCIATED CONTENT

Supporting information (PDF): general procedures, ^{1}H, ^{13}C and ^{19}F NMR spectra, theoretical methods, cartesian coordinates of the computed structures. The corresponding files are available free of charge.

AUTHOR INFORMATION

Corresponding Author

*E-mail: guillaume.lefevre@chimieparistech.psl.eu

Author Contributions

The manuscript was written through contributions of all authors. All authors have given approval to the final version of the manuscript.

Notes

The authors declare no competing financial interest.

ACKNOWLEDGEMENTS

This work has been financially supported by the joint program PheroChem (CNRS / M2i Company). The M2i Company is thanked for CIFRE PhD grants to E. Z. and P. C.; we also thank the “Fondation de la Maison de la Chimie” for a post-doctoral grant to N. L.; G.L. thanks the ERC (Project DoReMI StG, 852640) and the CNRS (Project IrMaCAR) for their financial support. The PSL Research University is thanked in frame of the NIMCOS project. The NMR shared facilities of Chimie ParisTech (Dr. M.-N. Rager) are thanked for technical support. G.L. dedicates this article to the memory of Prof. Gérard Cahiez, who initiated this collaborative work in 2018.

TOC graphic

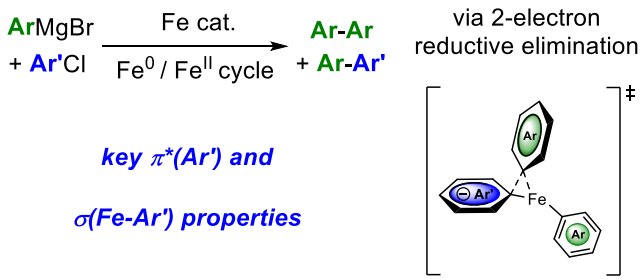
ArMgBr
+ Ar'Cl
Fe cat.
Fe0 / FeII cycle
Ar-Ar
+ Ar-Ar'
via 2-electron
reductive elimination
key π*(Ar') and
σ(Fe-Ar') properties
Ar
Ar'
Fe
Ar
‡